



Haoyang Mi¹, Chang Gong¹, Jeremias Sulam^{1,2}, Elana J. Fertig^{1,3}, Alexander S. Szalay^{4,5}, Elizabeth M. Jaffee^{3,6}, Vered Stearns³, Leisha A. Emens⁷, Ashley M. Cimino-Mathews^{3,8}, Aleksander S. Popel^{1,3}

¹Department of Biomedical Engineering, ²Mathematical Institute for Data Science, ³Sidney Kimmel Comprehensive Cancer Center, ⁴Department of Physics and Astronomy, ⁵Department of Computer Science, ⁶The Bloomberg~Kimmel Institute for Cancer Immunotherapy, ⁷Department of Pathology, Johns Hopkins University, U.S.A; ⁸Department of Medicine/Hematology-Oncology, University of Pittsburgh Medical Center, U.S.A

Introduction

- Overwhelming evidence has shown the significant role of the **tumor microenvironment (TME)** in governing the **triple-negative breast cancer (TNBC)** progression^[1].
- Image analysis and spatial statistics show promising results when applied to CD8+ T cells^[2], but quantitative analyses of **other important markers** and their correlations has not until now been possible.

Objectives

- In this study, we propose a novel and comprehensive workflow for characterizing the spatial arrangements of five immune markers (CD3, CD4, CD8, CD20, and FoxP3) by integrating **spatial model fitting, cluster morphometrics, and correlation analysis**

Materials and Methods

- Materials:** Digitally scanned slides from pathology archives at Johns Hopkins Medical Institutions.
- Computational workflow:** nuclei in IHC whole slide images are segmented to capture spatial locations¹. Afterwards, we convert such information to spatial point patterns and fed to the downstream submodules to quantify intra- and inter-tumoral heterogeneity.

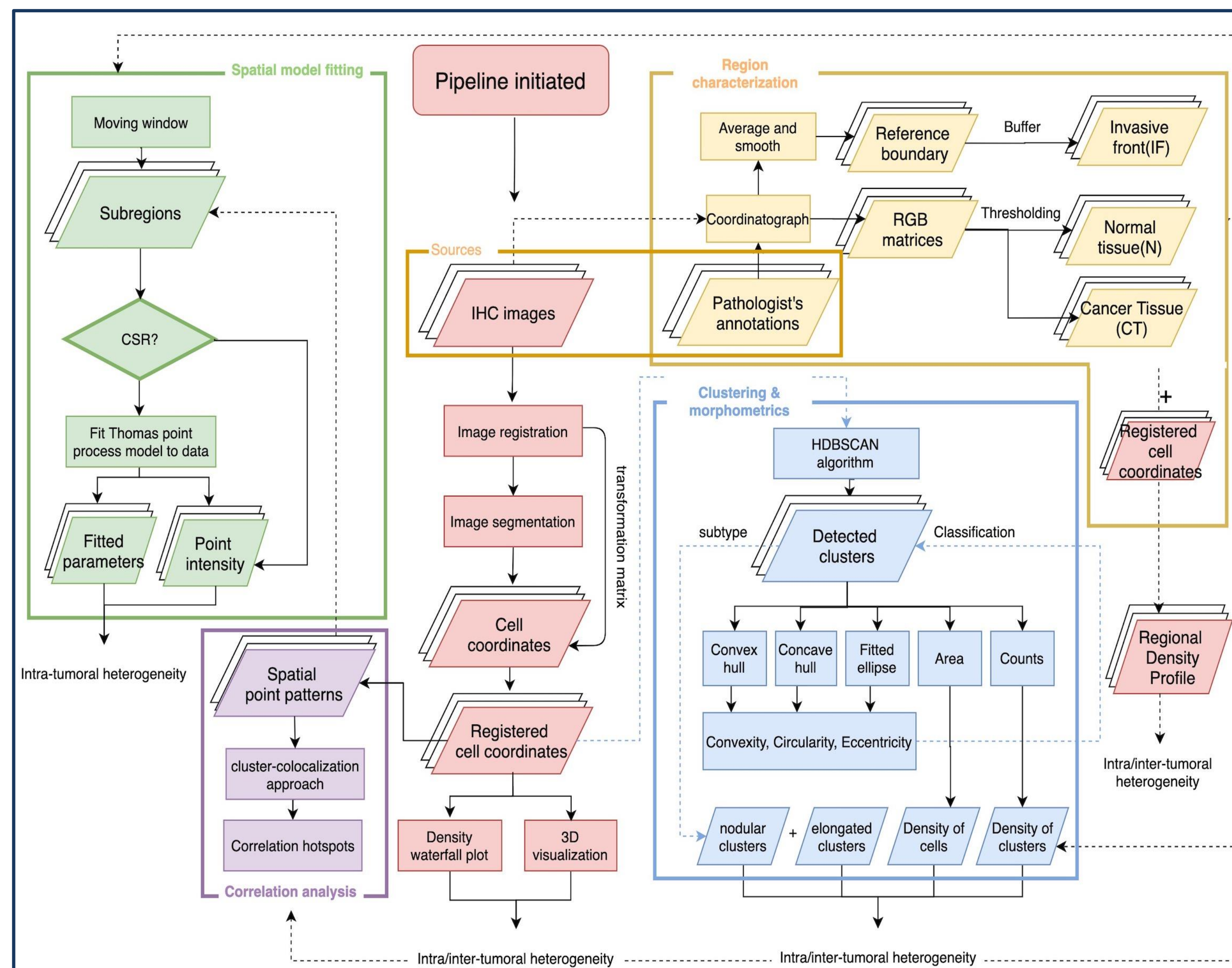


Figure 1. Diagram of the computational workflow

Results

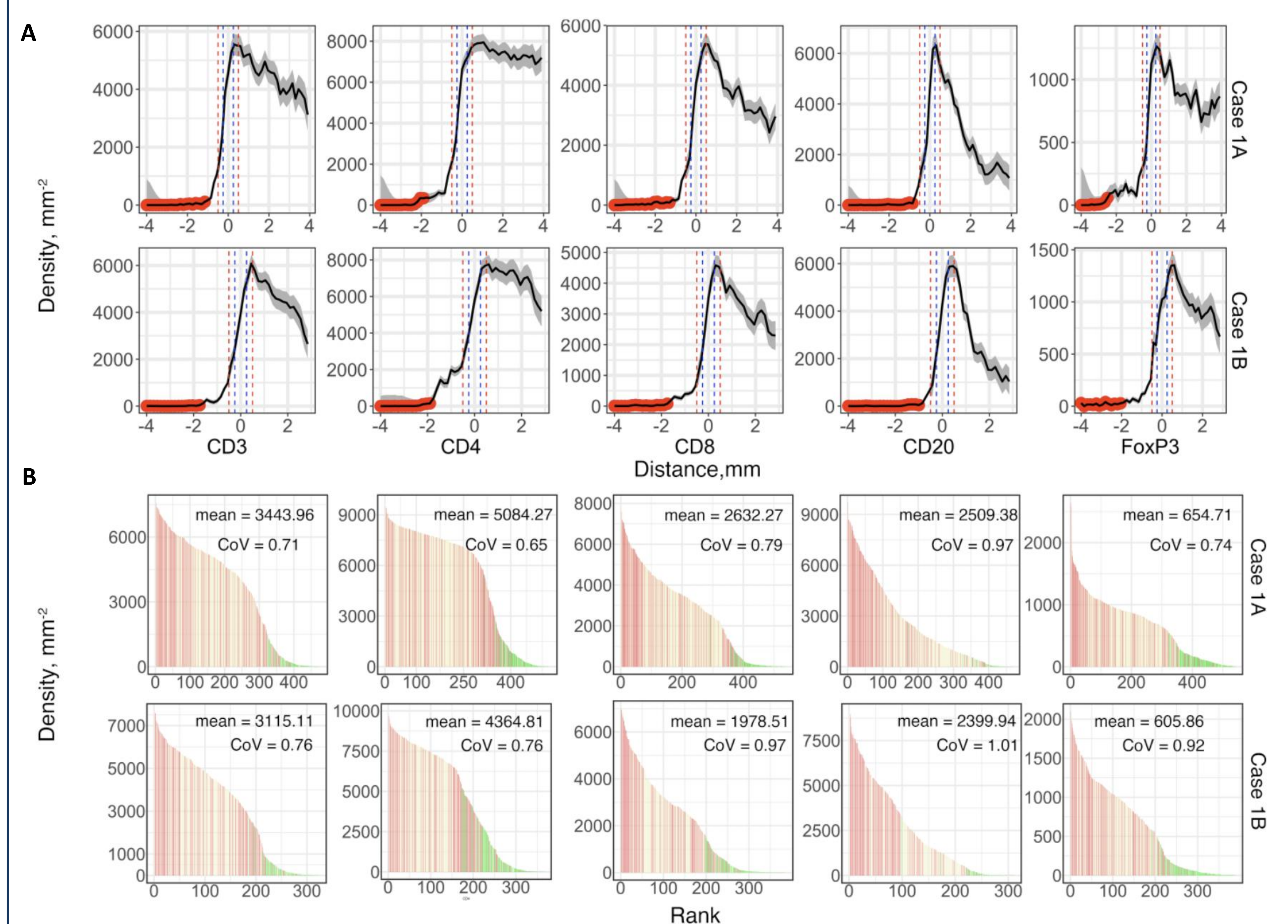


Figure 2. Cell density-distance profiles for Cases 1A and 1B. Whole tissues are segmented into equidistant sections. (A) Densities of different immune markers are calculated for each section and mapped with their distances to the invasive boundary, respectively. 95% confidence intervals are calculated upon the profile, and we use 80% of the density as the threshold to label those unreliable locations (red dots). Two definitions of IF are indicated as vertical lines, blue: width of 0.5mm; red: width of 1mm. (B) Densities of subregions are visualized using waterfall plots. For each slide, the densities are shown as bar heights, which are ranked from highest to lowest with colors corresponding to their locations. Color codes are consistent with (A).

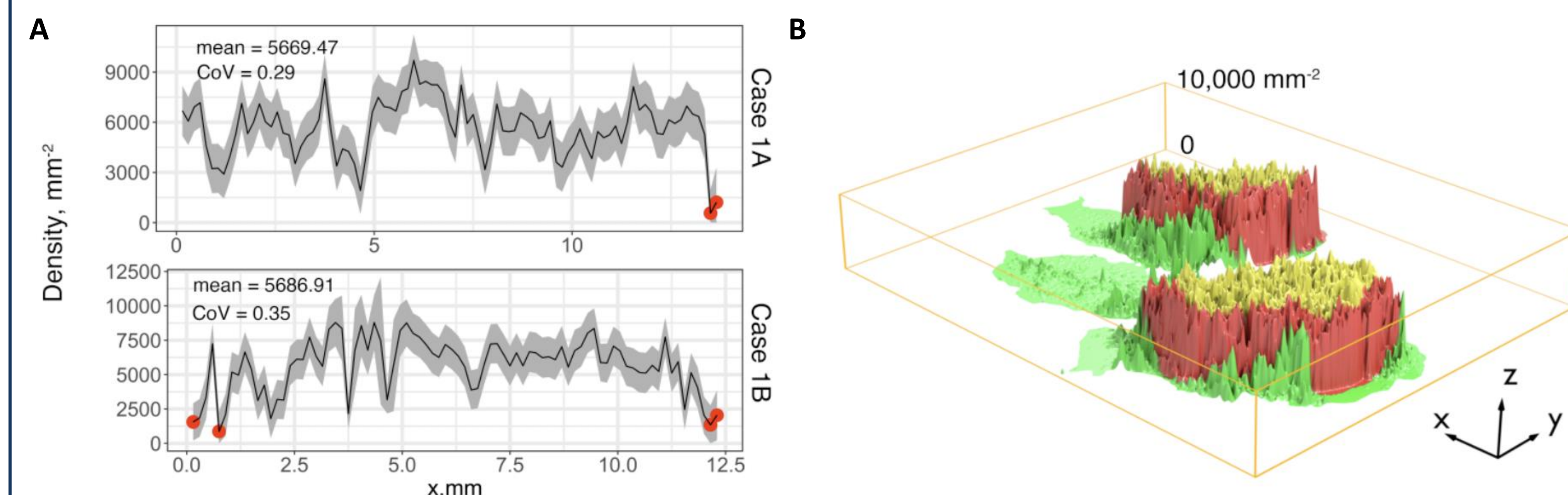


Figure 3. Cell density-distance profiles in IF. (A) The invasive front with thickness of 1mm is sectioned along its horizontal direction, and the same process is repeated to construct the cell density-distance profile. (B) 3D visualization for the density of each subregion with location labels. Color codes: central tumor (yellow), invasive front (red), and normal tissue (green).

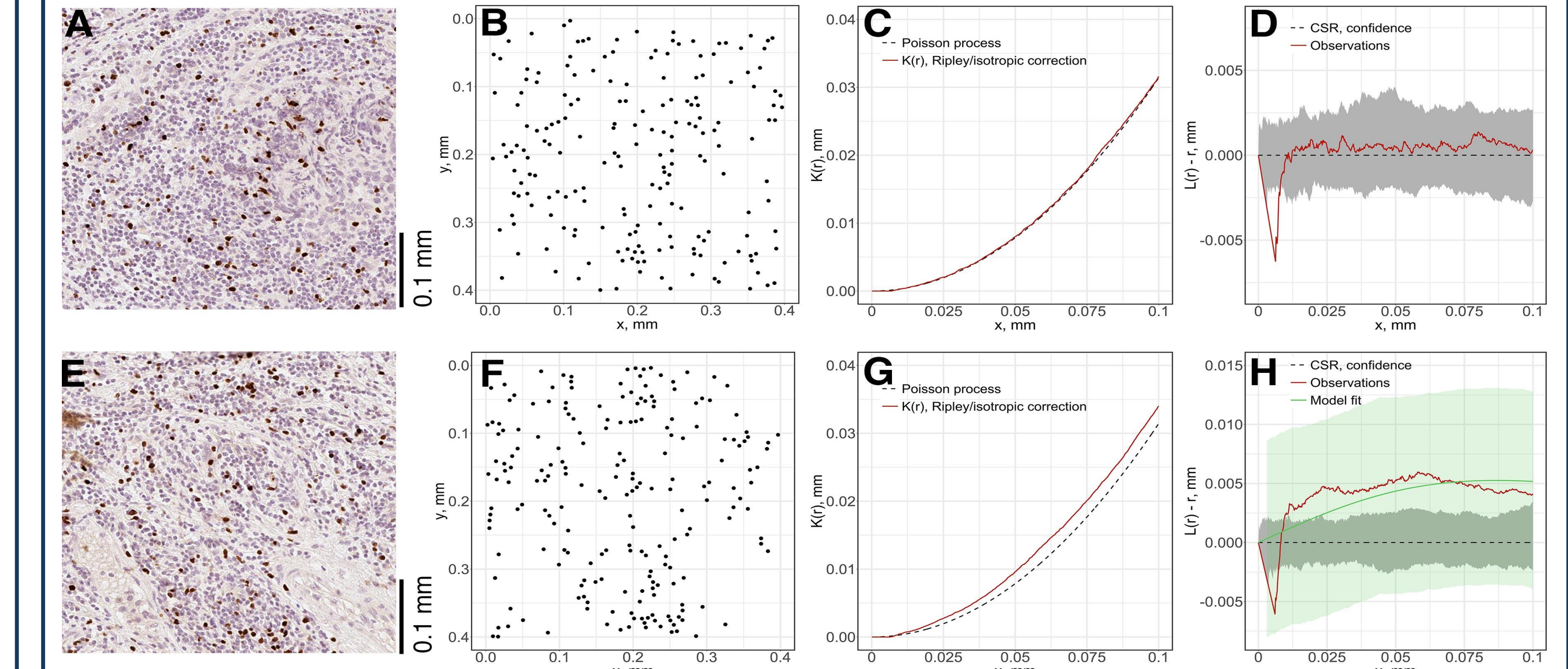


Figure 4. Local spatial point pattern analysis for subregions. (A)(E) Original exemplar IHC subregions; (B)(F) Associated point patterns. (C)(G) K-estimation using Ripley's border correction. (D)(H) L-transformation of K function and 95% confidence interval. Results are evaluated using Dao-Genton goodness-of-fit test (green envelope).

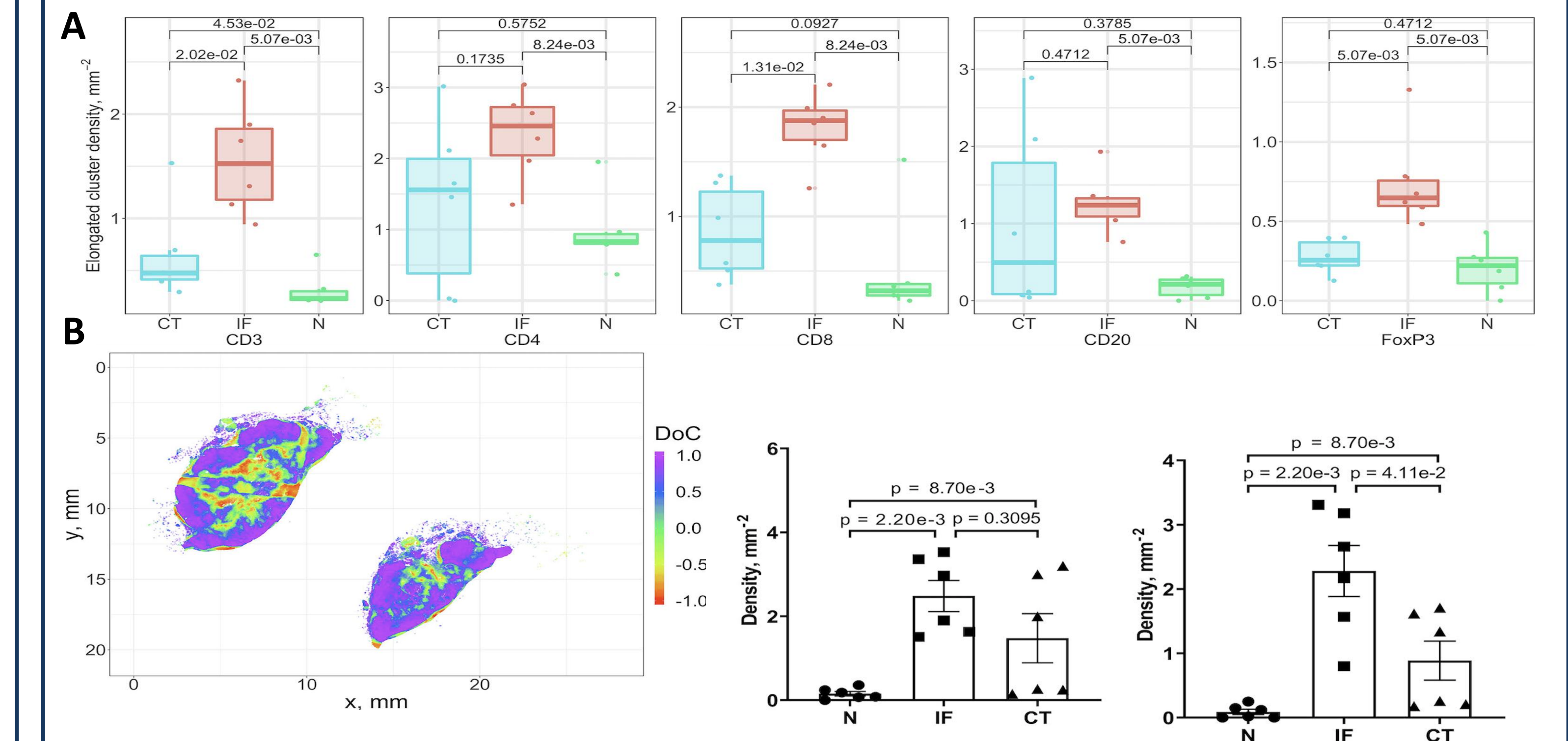


Figure 5. Clustering morphometrics and correlation analysis. (A) Distribution of elongated clusters; Elongated cluster is defined as: convexity < 0.3, or circularity < 0.3, or eccentricity > 0.9. (B) Correlation map of CD4+/FoxP3+ marker pair for Cases 1A (left island) and 1B (right island), and distribution of correlation clusters (evaluated by Wilcoxon rank-sum test).

Conclusion

- Results suggest a distinct role of IF in the tumor immuno-architecture. Importantly, the value of the workflow also lies in its potential to be linked to treatment outcomes and identification of predictive biomarkers for responders/non-responders, and its application to parameterization and validation of computational immuno-oncology models. Please refer to our published article for full information^[3].

References

[1] Klemm, F., and Joyce, J.A. (2015). Microenvironmental regulation of therapeutic response in cancer. *Trends in cell biology* 25, 198-213. doi: 10.1016/j.tcb.2014.11.006.
 [2] Gong, C., et al. (2018). Quantitative Characterization of CD8+ T Cell Clustering and Spatial Heterogeneity in Solid Tumors. *Frontiers in oncology* 8, 649. doi: 10.3389/fonc.2018.00649
 [3] Mi, H., et al. (2020). Digital pathology analysis quantifies spatial heterogeneity of CD3, CD4, CD8, CD20, and FoxP3 immune markers in triple-negative breast cancer. *Frontiers in Physiology*, 11:583333. doi: 10.3389/fphys.2020.583333